

---

**Paritat Muanchan<sup>1</sup>**

**Takashi Kyotani<sup>2</sup> and Hiroshi Ito<sup>1\*</sup>**

<sup>1</sup>Research Center for GREEN Materials and Advanced Processing (GMAP),  
Graduate School of Organic Materials Science, Yamagata University, Japan

<sup>2</sup>Institute of Multidisciplinary Research for Advanced Materials, Tohoku University, Japan

hiroshi@yz.yamagata-u.ac.jp

---

## **Vertically Aligned Composite Nanostructures Obtained by Nanoimprint Process**

### **Introduction**

Recently, polymer nanostructures have appeared based on structure-mediated surface functionalities produced by polymer nanoengineering. For example, it was found that the hydrophobic surface of cicada wing is covered with nanopillars which penetrate and consequently kill *Pseudomonas aeruginosa* within several minutes of adhesion [1]. To enhance the killing performance, characteristics and surface properties of VANs is necessary to improve; (1) hydrophobic properties, (2) surface areas, and (3) bacteria adherent or friction properties. Therefore, vertically aligned nanostructures (VANs) with ultra-high aspect ratio has attracted attention with greater hydrophobic, ultra-high surface area (aspect ratio), and higher friction properties. However, the low mechanical properties of VANs due to scaling down effect to nanostructures. To solve this problem, vertically aligned composite nanostructures (VACNs) using graphene can be used to replace the VANs which is not only to improve the mechanical properties but also can be proposed the multi-functional properties such as the excellent conductive performance (electrical and thermal) and chemical resistant [2].

Nanoimprint lithography using anodic aluminum oxide (AAO) template is currently available technology to prepuce the VANs which has gone into the methods faster, cheaper, higher-precision, less toxic, and more scalable as compared with solvent wetting method [3]. Here, we aim to investigate the nanoimprint process with AAO to produce VACNs. The material model used of polymer nanocomposites of polystyrene (PS) and graphene nanoplatelets (GPNs). In this work, the effect of GPNs contents on the flowing ability of PS, mechanical properties, thermal properties and surface properties (water contact angle measurement and friction coefficient) have been experimentally measurement and clarify.

### **Experimental**

Commercial grade PS (glass transition temperature ( $T_g$ ) = 87 °C, GPPS 679; PS Japan Corp.) and GPNs (6-8 nm-thick, 5  $\mu\text{m}$ -wide (10–15 w/w% < 100 nm), G0499, Tokyo Chemical Industry Co., Ltd.) were used in this study. PS–GPNs composites were prepared by solvent method [4] with the GPNs composition 1.0–5.0 w/w%. After that polymer films 500  $\mu\text{m}$ -thickness were fabricated by hot/cold press methods.

VACNs were prepared by thermal nanoimprint (Izumi Tech., Japan) using AAO template with the pore diameter of 100 nm and depth of 120–130  $\mu\text{m}$ . The PS–GPNs composite film was covered on AAO template and inserted into nanoimprint machine at temperature 120–180 °C for 5 min. After that, the polymer composite was driven through AAO by imprint pressure of 5.0 MPa for 30 min. The AAO was selectively removed by NaOH solution.

Surface morphologies of AAO and VACNs were observed by scanning electron microscope (SEM, TM-1000; Hitachi High-Tech). Thermal properties and mechanical properties were analyzed by using differential scanning calorimetry (DSC, TA-Instruments, DSCQ200), ai-Phase Mobile 1 (ai-Phase Co., Ltd.), and nanoindenter (Agilent Nano Indenter G200, Agilent Technologies, Inc.) respectively. Polymer melt droplet angle and water droplet angle were measured by droplet angle measurement machine (DM500, Kyowa Interface Science). Friction coefficient was measured by friction and wear tester (EFM–III–F, Orientec).

## Results and Discussion

In this study, the VANs and VACNs can be produced by thermal nanoimprint using AAO template. The nanopillar arrays and nanofiber arrays was obtained depend on the length of nanostructures. The result reveals that the length of the VANs/VACNs greatly depends on imprint temperature. The increases VANs/VACNs length by increasing the imprint temperature due to the reduction of polymer viscosity and surface tension at nanoscale [3]. The increased GNPs nanofilled content influences the reduction in the flowing ability within AAO pore due to the flowing resistance caused by geometric of the nanoplatelets.

The increase of GNPs composition has the result in the increases  $T_g$  of polymer bulk films and obtained nanostructures 87.1–101.5 °C due to the strongly adsorbing surface between PS and GNPs [5]. Moreover, we found that the relative of  $T_g$  between bulk films and the obtained nanostructures was increased 0.9–4.0 °C when increasing the GNPs composition. The thermal conductivity of obtained nanostructures was also increased 0.10–0.36 W/m.K due to the increase of GPNs composition.

Moreover, the addition of GNPs and the confinement effect within AAO can be enhanced the indentation modulus and indentation hardness of the obtained nanostructures from 0.10 to 1.10 GPa and 0.01 to 0.03 GPa respectively (see Fig. 1). The hydrophobic property of the obtained VANs and VACNs about 132.4° and 133.1° were observed. The increased friction coefficient of VACNs (0.48–0.61) as compared with VANs (0.38–0.47) was also observed.

## Acknowledgement

This work was supported by JSPS Grant-in-Aid for Scientific Research (C), project ID 16K06740.

## References

- [1] M. N. Dickson, E. I. Liang, L. A. Rodriguez, N. Vollereaux, A. F. Yee, *Biointerphases* 10(2) (2015) pp. 021010 (1–8)
- [2] J. J. Hernández, M. A. Monclús, I. Navarro-Baena, F. Viela, J. M. Molina-Aldareguia and I. Rodríguez, *Scientific Reports*, 7 (2017), pp. 43450 (1–10)
- [3] P. Muanchan, S. Suzuki, T. Kyotani and H. Ito, *Polymer Engineering and Science*, 57(2) (2017) pp. 214–223
- [4] N. Heeder, I. Chakraborty, A. Bose and A. Shukla, *Journal of Dynamic Behavior of Materials*, 1(1) (2015) pp. 34–54
- [5] K.-H. Liao, S. Aoyama, A. A. Abdala and C. Macosko, *Macromolecules*, 47(23) (2014) pp. 8311–8319

## Figures

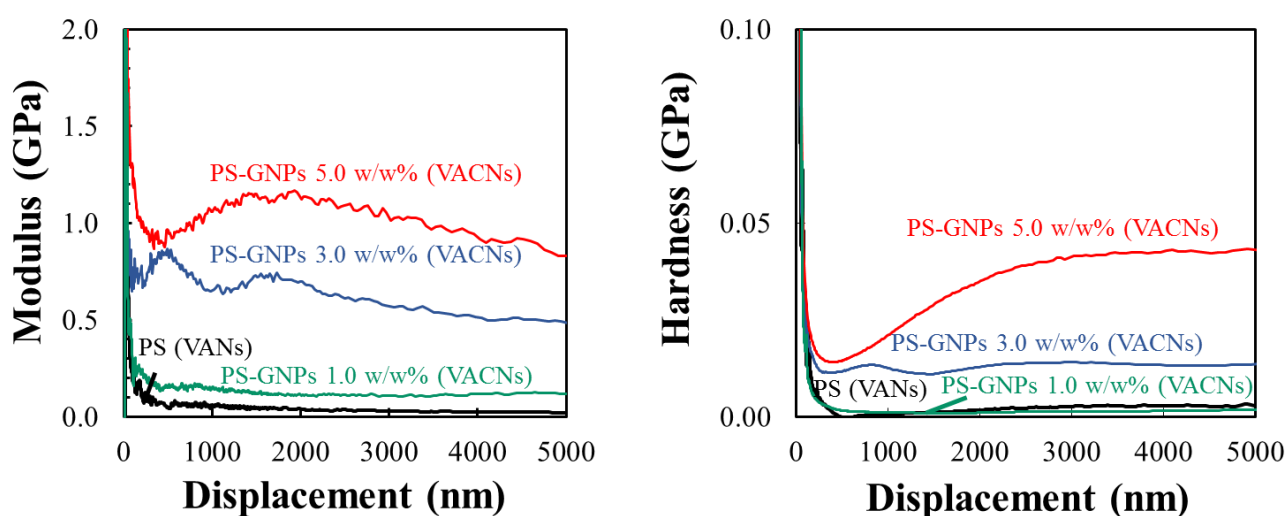


Figure 1: Indentation test results of VANs and VACNs